Proceedings of 2001 Korea-Japan Joint Seminar
on Particle Image Velocimetry
Seoul National Univ., Dec. 3 - 4

Measurements of a microchannel flow using micro-PIV

Inwon Lee*, Jayho Choi** and In-Seop Lee***

Key Words : Micro-PIV, MEMS, microfluidic elements, microchannel, micronozzle

Abstract

A micro-PIV(particle image velocimetry) measurement has been conducted to investigate flow fields in such microfluidic devices as microchannels and micronozzle. The present study employs a state-of-art micro-PIV system which consists of epi-fluorescence microscope, 620nm diameter fluorescent seed particles and an 8-bit megapixel CCD camera. Velocity vector fields with a resolution of 6.8 × 6.8 μm has been obtained, and the attention has been paid on the effect of varying measurement conditions of particle diameter and particle concentration on the resulting PIV results. In this study, the microfluidic elements were fabricated on plastic chips by means of MEMS processes and a subsequent molding process. Flow fields in a variety of microchannels as well as micronozzle have been investigated.

1. Introduction

Recently, much interest has been focused on the development of the microfluidic devices fabricated by means of MEMS (microelectromechanical system) technology. The microfluidic devices are employed in a various engineering and biomedical applications. Typical examples are micro-heat exchanger, micro-engine, micro-pump, DNA-chips and micro-TAS (Total Analysis System). These devices generally consist of such microfluidic elements as microvalve and microchannel for control of fluid flow. The main objectives of the miniaturization are the precise control of flow and the enhancement of reaction rate. Therefore, it is of great importance to gain clear understanding of flow phenomena inside the microfluidic components.

A literature survey reveals that researches on the characteristics of the flow inside a microchannel have been mainly dedicated to the measurement and prediction of the relation between the flow rate and the pressure loss [(1)-(4)]. It was reported that the measured pressure loss in a microchannel flow was larger than the predicted value using a macroscale laminar flow theory. This was then attributed to the roughness of the microchannel. However, there is no agreement between the various results regarding the flow rate-pressure loss relation in the simplest microfluidic elements with various results conflicting with each other. The understanding of the microscale flow phenomena is still far from being satisfactory, and more accurate measurement methodology is required. Most existing measurement techniques related to microfluidic devices are mainly for the global flow characteristics. Since it is local flow property that governs the overall efficiency of the microfluidic devices, the application of micro-PIV is highly desirable.

PIV (Particle Image Velocimetry) is a quantitative flow visualization method where the velocity vector fields can be obtained by processing the particle images of macroscale flow field [(5)(6)]. Recently, Santiago et al. [(7)] and Meinhart et al.[(8)] developed a micro-PIV system to obtain microscale resolution of the velocity vector field inside a microchannel flow. In these studies, 300nm-diameter epi-fluorescent flow-tracing particle and a microscope were employed in connection with the conventional PIV system.

In this study, flow field inside a variety of microfluidic elements was measured using a micro-PIV system.

* inwonlee@lge.com Digital Appliance Laboratory, LG Electronics Inc.
** jayho@lge.com Digital Appliance Laboratory, LG Electronics Inc.
*** islee@lge.com Digital Appliance Laboratory, LG Electronics Inc.

Microfluidic elements including microchannels and micronozzle were fabricated by means of MEMS process and measurements were performed for the Reynolds number ranges up to 20.

2. Experimental Apparatus

2.1 Micro-PIV

The detailed principle and outline of micro-PIV is described in Santiago et al. [7] and Meinhart et al.[8]. One of the main distinctions between the micro-PIV and the conventional macro-PIV is the size of the flow-tracing particle, in that submicron particle is utilized for tracking microscale flow field. The typical range of particle diameter is 100-300 nm. In this case, the wavelength of the incident light (532nm, for example) is longer than the particle diameter, so the intensity of the scattered light from the particle becomes too weak. Another difficulty arises from the illumination, because it is impractical to make a sufficiently 'thin' light sheet from the convectional light-sheet forming optics. Thus, a 'volume illumination' is inevitable. The weak, elastically scattered light is liable to be buried in the background light. Therefore, in micro-PIV, an inelastic scattering technique called epi-fluorescence was proposed by Santiago et al. [7]. This method utilizes polystyrene particles doped with fluorescent dye, with the emitted wavelength from the particle being different from the incident wavelength. In this study, 620nm-diameter fluorescent particles were employed. This particle incorporate a fluorescent dye which is tuned for the incident light from the Nd:YAG laser (λ=532nm), with the peak excitation wavelength of 542nm and the peak emission wavelength of 612nm.

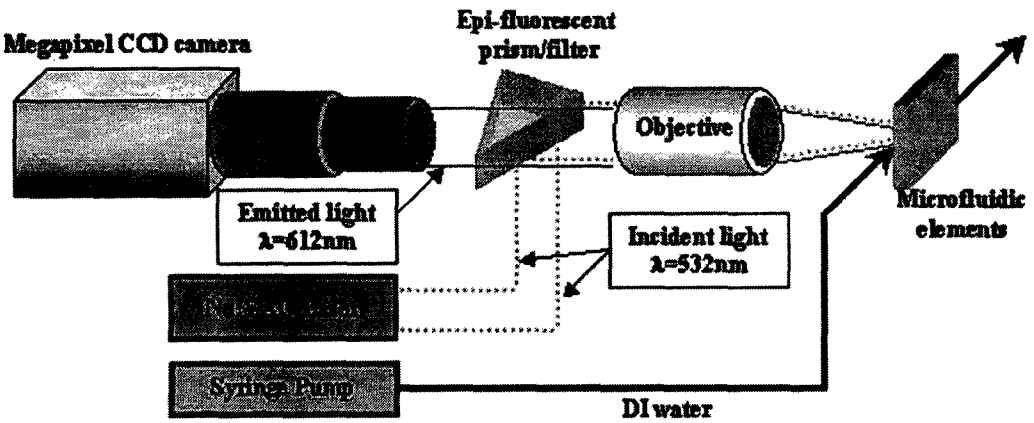

Fig. 1 Schematic diagram of micro-PIV system

The schematic diagram of the present micro-PIV system is illustrated in Fig. 1. The incident light for the illumination of the microfluidic element was generated from a two-head Nd:YAG laser with the maximum light energy of 300mJ. The incident light was guided through the epi-fluorescent prism and the 50X microscope objective lens. As mentioned earlier, the volume illumination was carried out in the present micro-PIV. The measurement domain in the out-of-plane direction was defined by the depth-of-field of the objective lens, which amounts to 0.9μm in the present apparatus. Figures 2 and 3 show the photographs of the present micro-PIV apparatus as well as the microfluidic element installed in the measurement rig.

Fig. 2 Photos of the present micro-PIV system

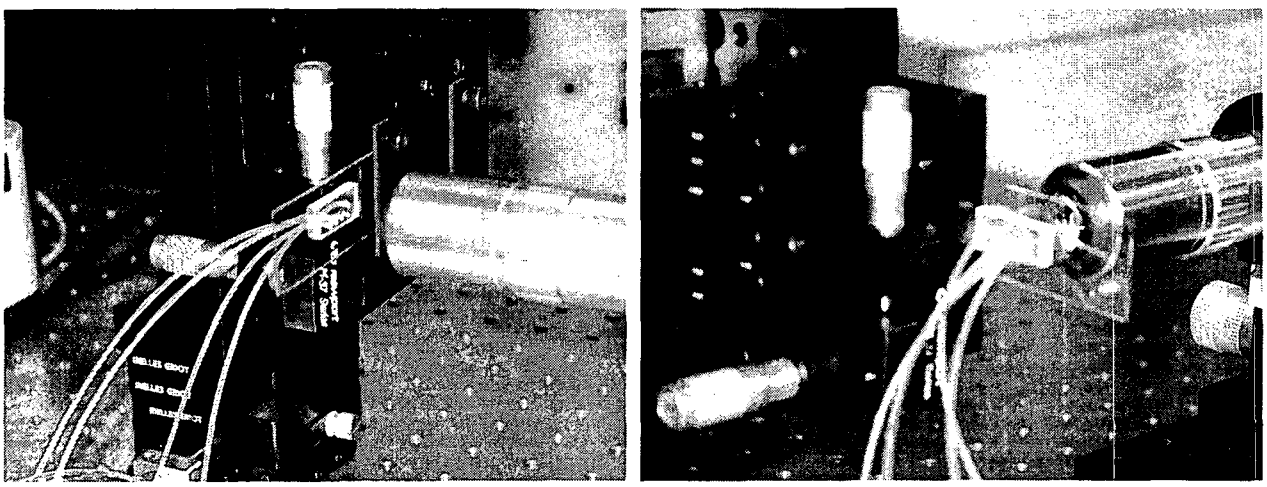

Fig. 3 Close-up photos of the present micro-PIV system

The emitted light (λ=612nm) from the particle is detected by a 8-bit CCD camera through a dichroic mirror and a bandpass filter. According to Meinhart et al.[8], The effective particle diameter on the CCD plane is estimated as follows;

$$d_e = \left[M^2 d_p^2 + d_s^2\right]^{1/2}, \quad d_s = 2.44M\frac{\lambda}{2NA} \qquad (1)$$

Here, M and NA is the magnification and the numerical aperture of the objective lens. d_p and λ represents the particle diameter (=620nm) and the wavelength of the emitted light (=612nm), respectively. For a magnification of M=50 and a numerical aperture of NA=0.55, the effective diameter amounted to d_e=74.9μm. This gives the particle size projected into the measurement plane of d_e/M=1.498μm. With the field of view in the present apparatus being approximately 430μm, one pixel size of the CCD amounts to the 0.425μm in the flow field. The particle size projected on the CCD plane corresponds to about 3.5 pixels. From the uncertainty estimate on the particle location given by Meinhart et al.[8], the measurement uncertainty equals to $\delta x \approx d_e/10M$=150nm.

The measurement depth is defined as the twice the distance from the center of the measurement plane

beyond which the particle image intensity is low enough to be neglected in the velocity measurement. According to Meinhart et al.[9], this is estimated as

$$\delta z_m = \frac{3n\lambda}{NA^2} + \frac{2.16nd_p}{NA} + d_p \qquad (2)$$

where n stands for the refractive index of the media. For the present non-immersed type (n=1), the measurement depth equals to δz_m= 9.18μm.

The instantaneous velocity vector fields were calculated from the two consecutive particle images illuminated by the double pulse of the Nd:YAG laser. The frame straddling time was adjusted between 2 and 30 microseconds in correspondence with the maximum velocity in the microchannel. The interrogation window size was 13.6×13.6 μm (32×32 pixels) and the resulting vector resolution was 6.8×6.8 μm for the 50% overlap.

2.2 Microfluidic Elements

The microfluidic elements used in this study were fabricated by MEMS processes. Firstly, a relief master is processed using onto the silicon wafer by the Wet Etch and Deep RIE methods. A polymer named PDMS (polydimethylsiolxane) was then cast into the mold to form engraved flow passages shown in Figs. 4-6. Lastly, a slide glass is bonded onto the PDMS using O_2-plasma bonding.

Three kinds of microfluidic elements, 300×50μm channel, 50×50μm channel and micronozzle with the contraction ratio of 5:1 in 300×50μm channel were made. As seen in the Figs. 4-6, the circular ports in the converging and diverging channel at the both ends of the channel are utilized as the inlet and outlet port. DI water flow in the microchannels is driven by the syringe pump which controls the flow rate in the ranges from 0.18 nl/s to 80 μl/s.

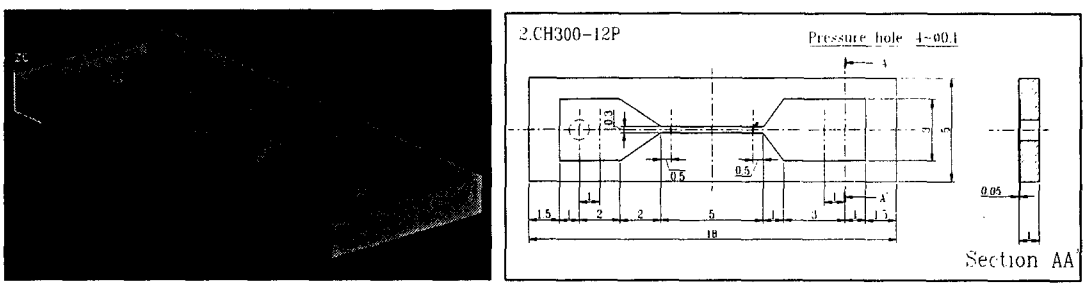

Fig. 4 Schematic drawings of 300μm×50μm microchannel

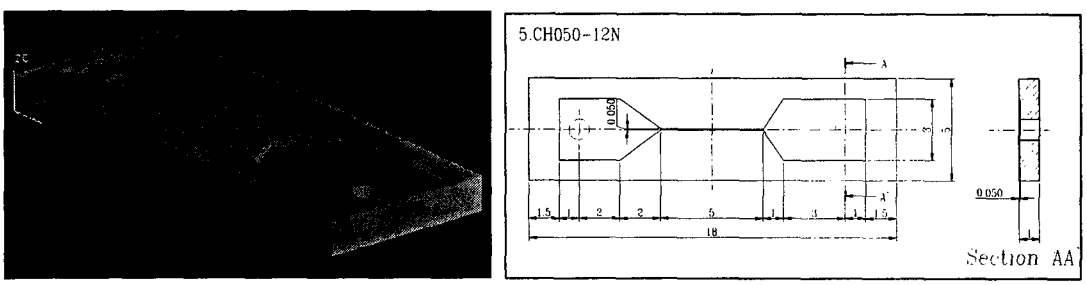

Fig. 5 Schematic drawings of 50μm×50μm microchannel

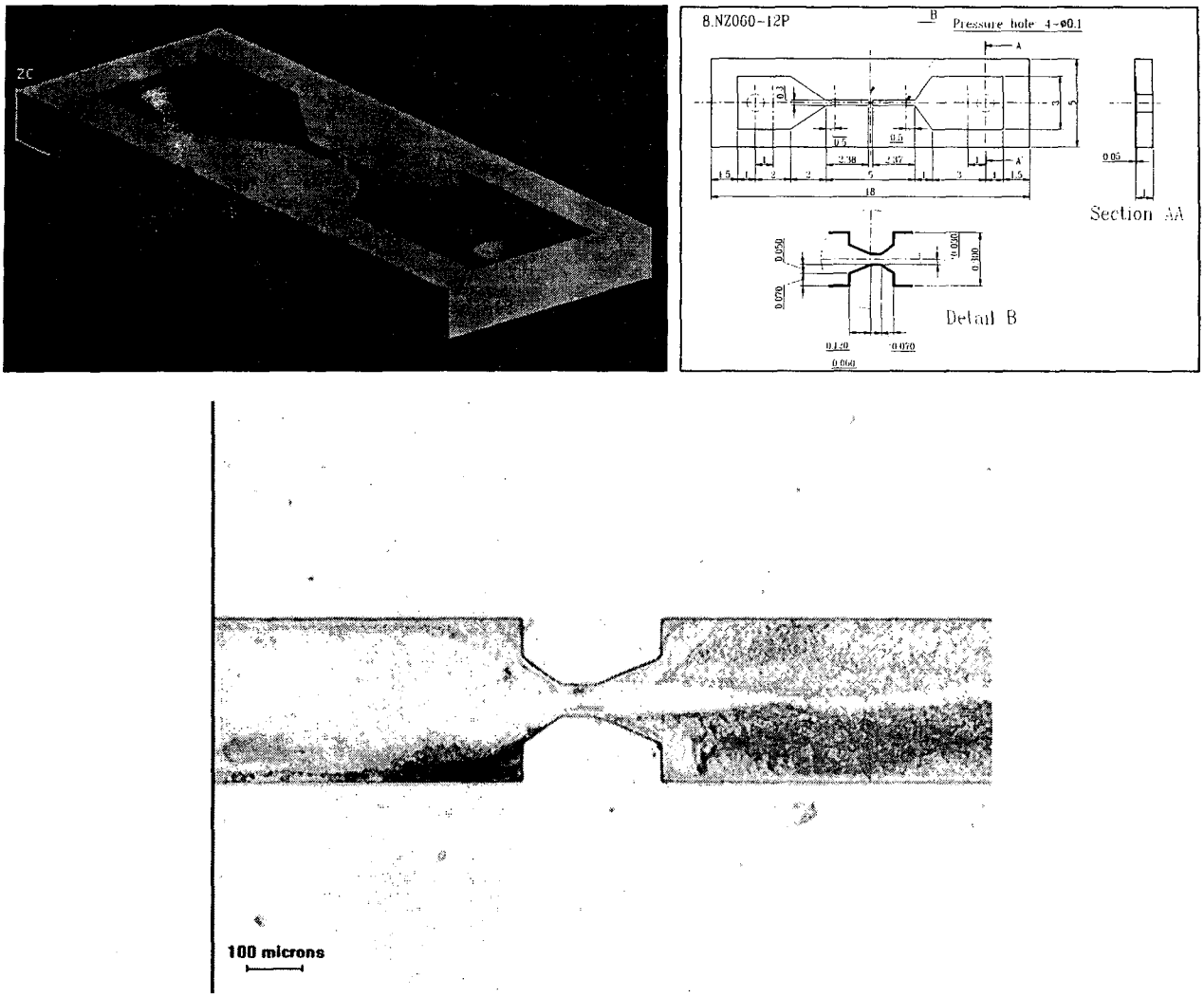

Fig. 6 Schematic drawings of the micronozzle

As shown in Fig. 3, the microfluidic elements were installed in the 3-axis tilt stage so that the measurement plane became parallel to the centerplane of the channel. A micron-resolution traverse was used to locate the measurement plane at the mid-span of the channel. The objective lens could be located so that the object plane was focused at both end planes of the channel and then traversed to the mid-span position.

The density of flow-tracing particle was set to volume fraction of 0.1% in the present measurement. Given the number density of the particle of 8.4×10^9/ml, there were 14.3 particles in 13.6μm ×13.6μm×9.2μm interrogation volume. This number of particle is considered sufficient for the velocity vector estimation using standard autocorrelation technique.

3. Experimental Results

The measurements in the present study were performed for 6 cases in which the width and the flow rate were changed, as shown in Table. 1. The flow rate was adjusted using the syringe pump. The average velocity V is defined as V=Q/A, with Q and A being the flow rate and the cross sectional area, respectively. In these cases, the Reynolds number Re is defined from the average velocity V and the hydraulic diameter D_h as $Re=VD_h/\nu$.

Case #	Element	Width [μm]	Depth [μm]	Hydraulic Diameter D_h [μm]	Flow rate Q [μl/s]	V [m/s]	Re
1	Microchannel	300	50	85.7	0.75	0.05	4.3
2	Microchannel	300	50	85.7	1.50	0.10	8.6
3	Microchannel	300	50	85.7	3.00	0.20	17.2
4	Microchannel	50	50	50	0.125	0.05	2.5
5	Microchannel	50	50	50	0.250	0.10	5.0
6	Micronozzle	300	50		0.500		

Table. 1 Measurement conditions

Fig. 7 shows the fluorescent particle images detected by the CCD camera. The ensemble averaged vector plots and contour plots of vorticity for cases #1-#3 in 300 × 50μm microchannel are plotted in Figs. 8-10. It is seen that for each case uniform flow, of which speed is nearly the same as the average velocity V, is developed in the central region of the channel. In addition, near wall profile is well observed.

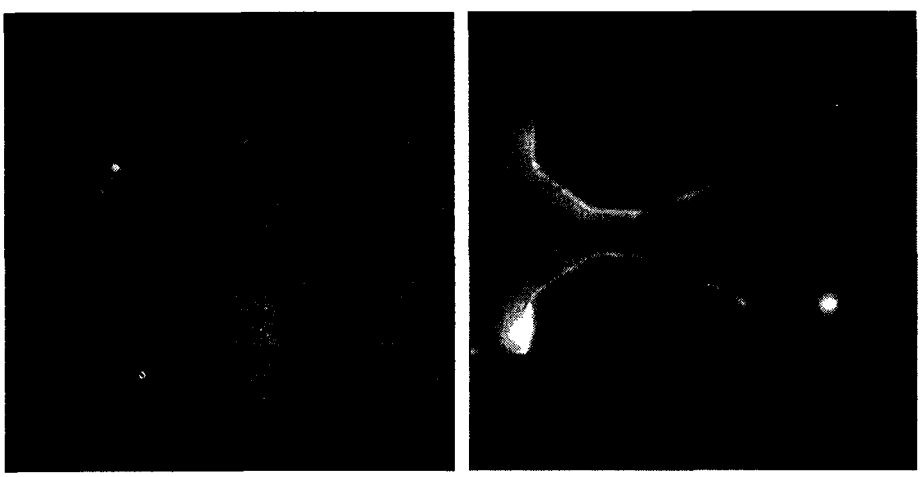

a) Case #2, 300 ×50μm microchannel b) Case #6, Micronozzle

Fig. 7 Particle Images of the present study

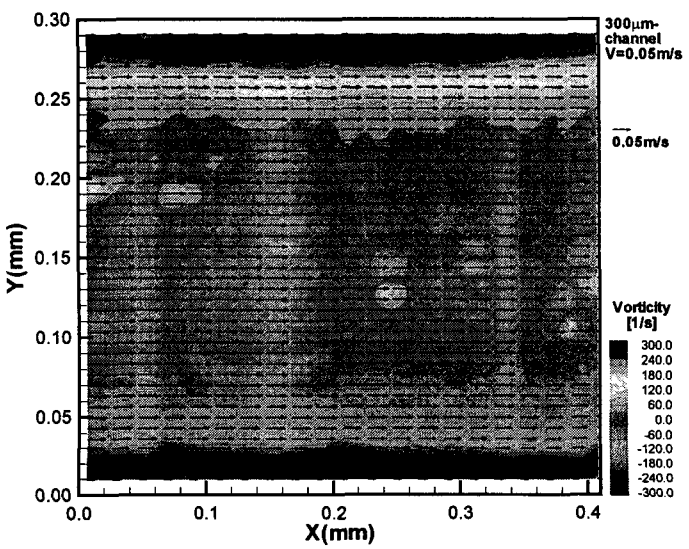

Fig. 8 Ensemble-averaged vector plot and contour plot of vorticity for Case #1

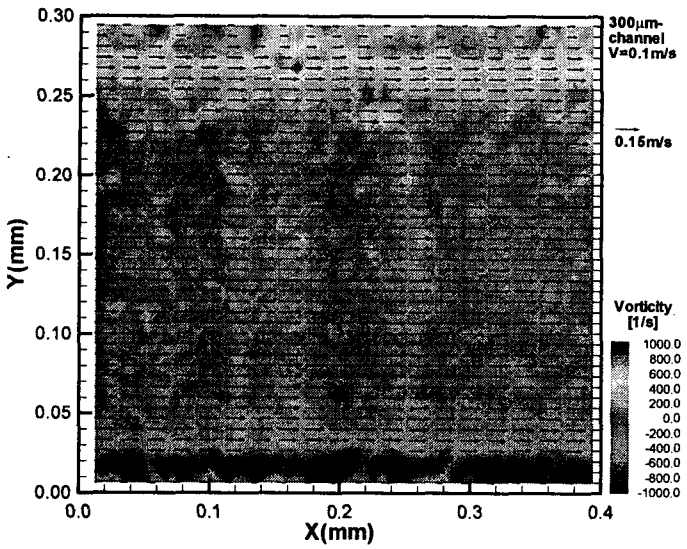

Fig. 9 Ensemble-averaged vector plot and contour plot of vorticity for Case #2

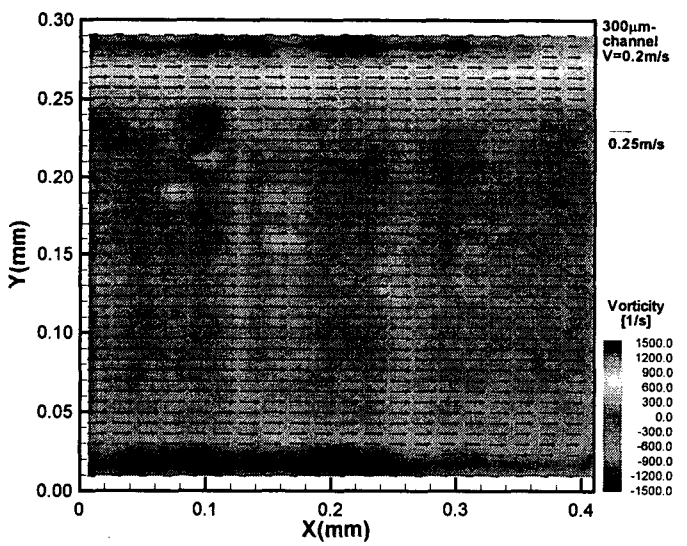

Fig. 10 Ensemble-averaged vector plot and contour plot of vorticity for Case #3

Fig. 11 exhibits the ensemble averaged vector plots and contour plots of speed for cases #4 and #5 in 50 × 50μm microchannel. In these cases, the field of view and the vector resolution are the same as those in the preceding cases. So the present resolution gives only the limited results for 50μm width microchannel. However, the parabolic profile is well observed in these cases. The parabolic profile indicates that the flow field becomes fully developed in these cases. This is contrary to the cases #1-#3 in 300× 50μm microchannel

For the micronozzle case (Case #6), the vector plot and vorticity contours are illustrated in Fig. 12. It is found that there is a considerable acceleration of the flow due to the contraction ratio of 5:1 of the nozzle. Figs. 13 and 14 are the profiles of the streamwise velocity, obtained by the line-averaging in the streamwise direction of the vector plots for Cases #1-#5. For 300 × 50μm microchannel in Fig. 13, the symmetry of the profile is clearly discernible. In addition, nearly parabolic profile can be found in Fig. 14 in spite of the insufficient vector resolution.

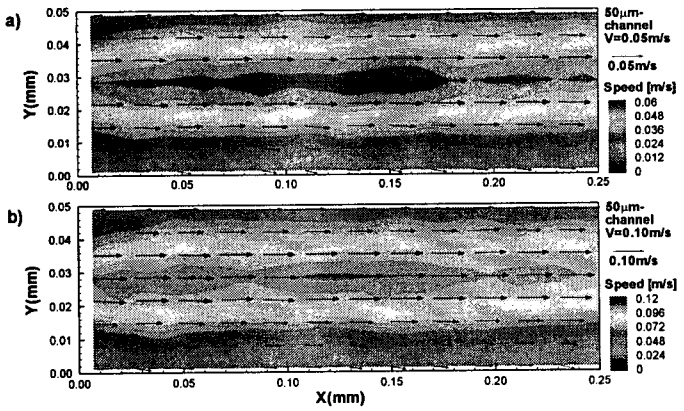

Fig. 11 Ensemble-averaged vector plot and contour plot of vorticity for Case #4 and #5

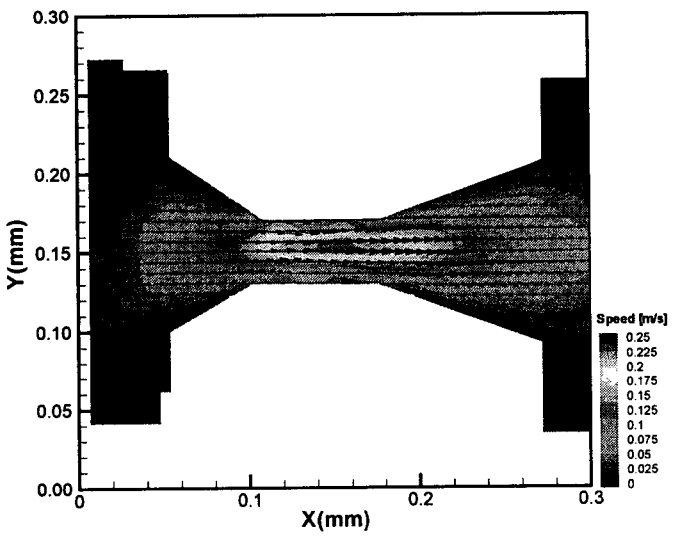

Fig. 12 Ensemble-averaged vector plot and contour plot of flow speed for Case #6

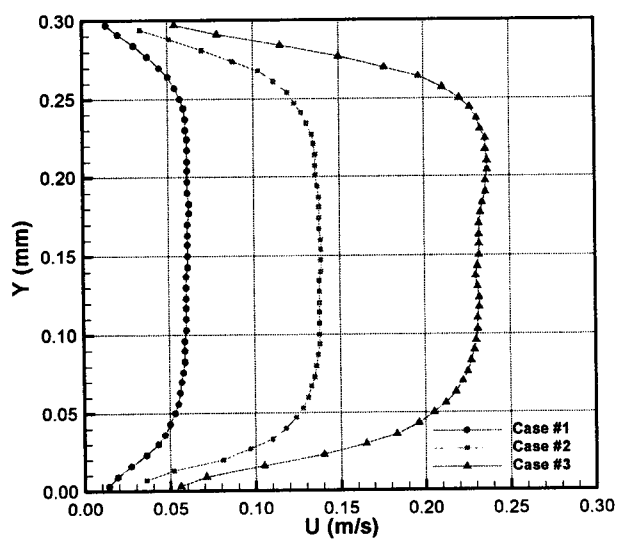

Fig. 13 Streamwise-averaged streamwise velocity profile for 300μm×50μm channel

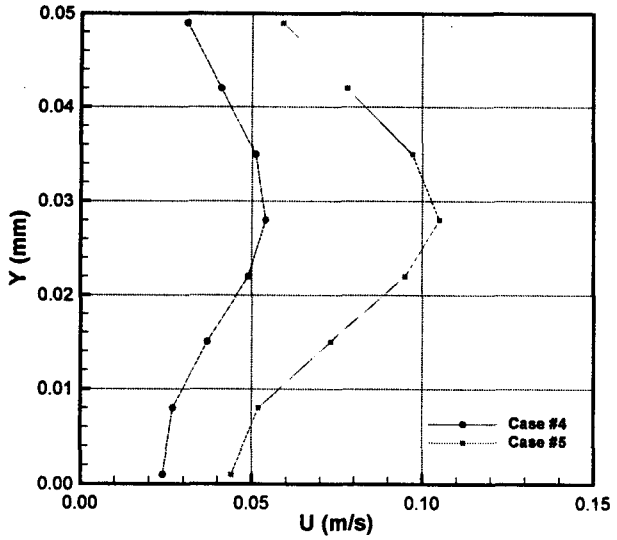

Fig. 14 Streamwise-averaged streamwise velocity profile for 50μm×50μm channel

4. Conclusions

In this study, flow fields inside microfluidic elements such as microchannels and micronozzle have been measured via a micro-PIV system. The microfluidic elements used in this study were fabricated from PDMS (polydimethylsiolxane) by MEMS processes. The present micro-PIV system consisted of epi-fluorescence microscope and 620nm-diameter fluorescent polystyrene particles. Using 50% overlap of the interrogation window, a velocity vector resolution of 6.8 × 6.8 μm was obtained with the maximum speed up to 0.25m/s.

References

(1) Harley, J. and Bau, H., 1989, "Fluid Flow in Micron and Submicron Size Channels," IEEE Trans. THO249-3, pp.25-28

(2) Pfahler, J. N., 1992, "Liquid transport in micron and submicron size channels," Ph. D. thesis, Dept.of Mechanical Engineering, Univ. of Pennsylvania

(3) Weilin, Q., Mala, G. M. and Li, D, 2000, "Pressure-driven water flows in trapezoidal silicon microchannels," Int. J. Heat Mass Transfer, vol.43, pp.354-364

(4) Mala, G. M. and Li, D., 1999, "Flow characteristics of water in microtubes," Int. J. Heat Fluid Flow, vol.20, pp.142-148

(5) Adrian, R. J., 1991, "Particle-imaging techniques for experimental fluid mechanics," Ann. Rev. Fluid Mech., vol.23, pp.261-304

(6) Lee, I. S., Kaga, A. and Yamaguchi, K., 1999, "Quantitative Evaluation of Gray Level Difference and Successive Abandonment Methods Using Artificial Visualized Images," Journal of Visualization Society of Japan, vol.19, pp.57-63 (in Japanese)

(7) Santiago, J. G., Wereley, S. T., Meinhart, C. D., Beebe, D. J. and Adrian, R. J., 1998, "A particle image velocimetry system for microfluidics," Exp. Fluids, vol.25, pp.316-319

(8) Meinhart, C. D., Wereley, S. T. and Santiago, J. G., 1999, "PIV measurements of a microchannel flow," Exp. Fluids, vol.27, pp.414-419

(9) Meinhart, C. D., Wereley, S. T. and Gray, M. H. B., 2000, "Volume illumination for two-dimensional particle image velocimetry," Meas. Sci. Tech., vol.11, pp.809-814